photonics

MDPI

Communication

A High-Sensitivity SPR Sensor with Bimetal/Silicon/Two-Dimensional Material Structure: A Theoretical Analysis

Pengyu Zhang [1,†], Junxian Wang [1,†], Guoquan Chen [1], Jian Shen [1,2,*], Chaoyang Li [1,2] and Tingting Tang [3]

[1] School of Information and Communication Engineering, Hainan University, Haikou 570228, China; pengyuzhang@hainanu.edu.cn (P.Z.); 20181685310051@hainanu.edu.cn (J.W.); 20191683310139@hainanu.edu.cn (G.C.); lichaoyang@hainanu.edu.cn (C.L.)
[2] Dongguan ROE Technology Co., Ltd., Dongguan 523000, China
[3] Information Materials and Device Applications Key Laboratory of Sichuan Provincial Universities, College of Optoelectronic Engineering, Chengdu University of Information Technology, Chengdu 610225, China; skottt@163.com
* Correspondence: shenjian@hainanu.edu.cn
† The first two authors contributed equally to this work.

Abstract: In this paper, we reported a theoretical study of a novel Surface plasmon resonance (SPR) biosensor composed of BK7 prism, gold (Au)/silver (Ag) bimetallic layer, silicon and two-dimensional (2D) materials. The bimetallic layer combines the advantages of Au and Ag and the high refractive index silicon layer enhances the electric field on the surface of the sensor, so that the sensor has a better overall performance in terms of sensitivity and figure of merit (FOM). Compared with ordinary dielectrics, 2D materials have excellent photoelectric properties, such as larger specific surface area, higher carrier density and stronger adsorption capacity, which improve the detection ability of the sensor. The sensitivity of the optimized sensor achieves 297.2°/RIU, 274°/RIU and 246°/RIU when the silicon layer is covered with graphene, MXene ($Ti_3T_2C_x$) and MoS_2, respectively. Compared with the traditional SPR sensor, the sensitivity of the structure has been significantly improved, and its excellent performance has broad application prospects in biosensing and other fields.

Keywords: surface plasmon resonance; bimetallic; 2D materials; silicon; sensitivity

Citation: Zhang, P.; Wang, J.; Chen, G.; Shen, J.; Li, C.; Tang, T. A High-Sensitivity SPR Sensor with Bimetal/Silicon/Two-Dimensional Material Structure: A Theoretical Analysis. *Photonics* **2021**, *8*, 270. https://doi.org/10.3390/photonics8070270

Received: 30 May 2021
Accepted: 4 July 2021
Published: 9 July 2021

1. Introduction

Surface plasmon resonance (SPR) is an optical phenomenon occurring at the interface between metal and dielectric. The surface plasmon wave excited under specific incident conditions is very sensitive to the change of the refractive index of the medium. SPR sensing technology has many advantages, such as being real-time, requiring no labeling, no damage, high sensitivity [1–5], etc., so it is widely used in biological [6,7], chemical [8–10], medical [11,12], food safety [13,14] and other fields. In general, an SPR sensor with gold as a metal layer has a better biological affinity, chemical stability and higher sensitivity, while an SPR sensor with silver as metal layer has a sharper resonance spectrum and higher detection accuracy [15], and its shortcomings of easy oxidation can be compensated by placing on its surface with Au, silicon or other dielectrics.

An important indicator of the SPR sensor is the adsorption capacity of the sensor surface for the analyte. In order to improve the performance of the sensor, different films have been used to coat the surface of the sensor. In recent years, 2D materials as a new type of material, have been favored by many researchers for their excellent photoelectric properties. Covering various 2D material films on the surface of SPR sensors has also become a hot research topic. For example, Wu et al. Covered the Au layer with graphene, resulting in a 25% sensitivity enhancement [16]. Wu L. et al. theoretically presented an SPR sensor; they covered MXene-Ti_3C_2Tx on Au and finally got the maximum sensitivity of

160°/RIU [17]. Kumar R et al. has proposed and performed the result analysis of silicon and MXene based SPR sensor, results show a sensitivity of 231°/RIU [18]. Varasteanu P used different 2D transition metal dihalides (MX_2, M stands for transition metal, X stands for halogen) to cover the surface of metal layer, so as to improve the sensitivity of the SPR sensor [19].

In recent years, the use of metamaterials and metastructures to excite SPR or for sensing has also been a hot topic [20,21]. Giovanna Palermo et al. explored the possibility of covering a metal surface with metamaterials to excite SPP and BPP modes [22]. Kabashin A.V. et al. demonstrate an improvement in biosensing technology using a plasmonic metamaterial that is capable of supporting a guided mode in a porous nanorod layer [23]. Kandammathe Valiyaveedu Sreekanth et al. developed a miniaturized plasmonic biosensor platform based on a hyperbolic metamaterial that can support highly confined bulk plasmon guided modes over a broad wavelength range from visible to near infrared [24]. Ruffato G. et al. studied nanogroups gold plasma structures for sensing applications [25]. These novel studies make SPR research more abundant and in-depth.

In this paper, an SPR biosensor based on Kretschmann structure is proposed in angle interrogation. Through the research and optimization of multilayer thin film materials, the innovative Au/Ag/Si/2D material structure greatly improved sensitivity of the sensor.

By optimizing thickness of the bimetallic and silicon layer, the sensitivity of 272.6°/RIU was achieved at 632.8 nm, which is about twice the sensitivity of a traditional bimetallic SPR sensor. On this basis, the sensing characteristics of silicon covered with different 2D materials are analyzed. Finally, it is found that silicon covered with double layer graphene has an ultra-high sensitivity of 297.2°/RIU. The performance of the sensor in wavelength modulation is also discussed at the end of this paper.

2. Model Design and Analysis of Principle

A five-layer structure composed of glass, Au, Ag, silicon, and 2D materials is our model (see Figure 1a). The incident light is a transverse magnetic wave with the wavelength of 632.8 nm. Unlike the common bimetallic SPR structure that covers the Au film on the Ag film, this device covers the Ag film on the surface of the Au film, and then covers the silicon on the Ag film. This cannot only avoid the oxidation of the Ag film, but also improve the sensitivity of the sensor. The electric field distribution in the article is simulated by COMSOL Multiphysics software. Figure 1b is the finite element simulation result of the magnetic field H_z component of the structure. Relative to the nano-scale thickness of the bimetallic layer, silicon layer and two-dimensional material, the thickness of the prism and sensing medium in the sensor and the size of the sensor in the x and y directions can be regarded as semi-infinite. The thickness of the bimetallic layer and silicon layer have been marked in Figure 1a. It can be seen from Figure 1b that the electromagnetic wave energy is concentrated on the interface between the 2D material and the sensing medium, which is conducive to detecting the change of the refractive index of the sensing medium.

We could apply the transfer matrix method to calculate the reflectance in multilayers. The form of wave equation in a medium characterized by $\varepsilon^{(\mathrm{n})}$ is

$$\mathbf{k}^{(\mathrm{n})2}\mathbf{E}_0^{(n)} - \mathbf{k}^{(\mathrm{n})}(\mathbf{k}^{(\mathrm{n})}\bullet\mathbf{E}_0^{(n)}) = \frac{\omega^2}{c^2}\varepsilon^{(n)}\mathbf{E}_0^{(n)} \tag{1}$$

Here, $\mathbf{k}^{(\mathrm{n})}$ is the complex wave vector and $\mathbf{E}_0^{(n)}$ is the complex amplitude of the electric field, c and ω denote the speed of light in vacuum and its angular frequency respectively.

According to the boundary condition of electromagnetic field, the electric field in each layer has the following relation

$$\mathbf{E}_0^{(0)} = \mathrm{Q}\mathbf{E}_0' \tag{2}$$

where $\mathbf{E}_0$ and $\mathbf{E}'_0$ represent the electric fields on the upper and lower surfaces of multilayer media respectively, and $\mathbf{Q}$ is the fourth-order transfer matrix connecting the electric fields of each layer, which can be expressed as

$$\mathbf{Q} = \mathbf{D}_0 \prod_{n=1}^{N} (\mathbf{D}_\mathrm{n}\mathbf{P}_\mathrm{n}\mathbf{D}_\mathrm{n}^{(-1)})\mathrm{D}'_0 \tag{3}$$

Here, $\mathbf{D}_\mathrm{n}$ and $\mathbf{P}_\mathrm{n}$ are the dynamic matrix and propagation matrix of the n-th layer of media, respectively. Then the reflection coefficient and reflectivity can be calculated as

$$r = \frac{Q_{11}Q_{43} - Q_{13}Q_{41}}{Q_{11}Q_{33} - Q_{13}Q_{31}} \tag{4}$$

$$R = |r|^2 \tag{5}$$

Here, Q_{ab} is the element in 4×4 matrix $\mathbf{Q}$.

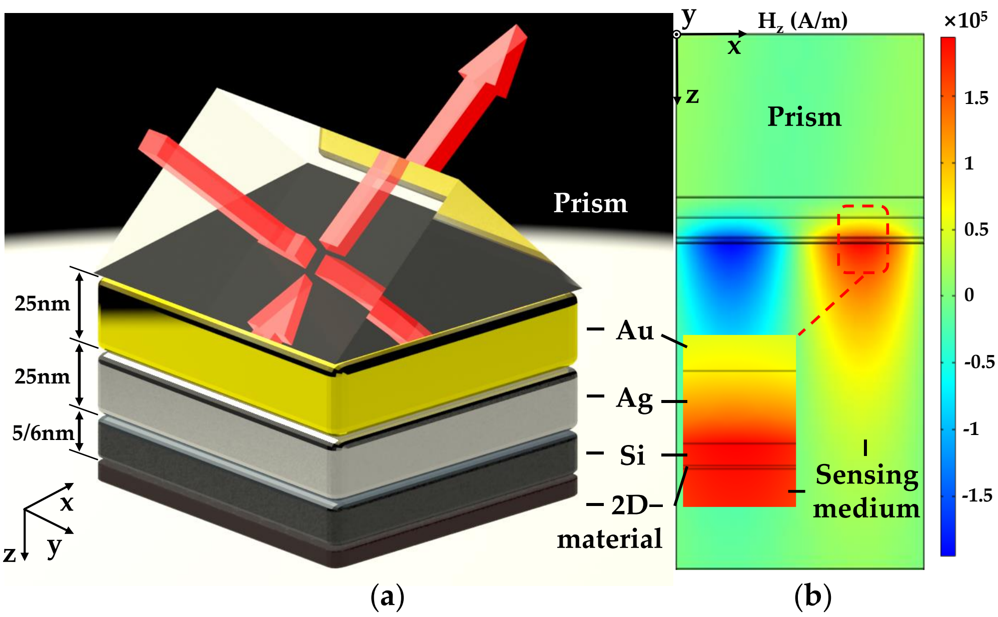

Figure 1. (**a**) Schematic diagram of the proposed SPR sensor. (**b**) Magnetic field in z direction.

For refractive index sensors, the sensing performances can be quantified by sensitivity (S), full width at half maximum (FWHM) and figure of merit (FOM). The sensitivity in angle interrogation and wavelength interrogation can be expressed as

$$S_\theta = \frac{\Delta\theta}{\Delta n} \tag{6}$$

$$S_\lambda = \frac{\Delta\lambda}{\Delta n} \tag{7}$$

$$FOM = \frac{S}{FWHM} \tag{8}$$

where $\Delta\theta$ is the change of resonance angle (in angle interrogation), $\Delta\lambda$ is the change of wavelength of incident light (in wavelength interrogation) and Δn is the change of refractive index of the solution to be measured. Higher sensitivity means that the sensor is more sensitive to the change of refractive index, and smaller *FWHM* means higher detection accuracy. *FOM*, defined by the $S/FWHM$, is a comprehensive evaluation of the sensor. The focus of this article is the sensitivity of the sensor.

In this paper, we mainly study the sensing characteristics of the designed sensor in angle interrogation. In addition, the influence of the incident angle on the sensing characteristics in wavelength interrogation is also discussed briefly. The incident light is a TM wave with a wavelength of 632.8 nm, and the refractive index of each layer is shown in Table 1 [26].

Table 1. Refractive index of each layer at 632.8 nm.

Layer	Materials	Refractive Index
Prism	BK7	1.5168
Bimetal	Au	0.14330 + 3.6080i
Bimetal	Ag	0.051255 + 4.3165i
Sensing medium	Water	1.33 + Δn

3. Simulation Results and Analysis

3.1. Influence of Thickness of Ag/Au Bimetallic Layer on SPR

In this section, we will analyze the impact of the type and thickness of metal on the performance of the SPR sensor. The sensor structure we are concerned with is a prism/Au/Ag/medium structure (Figure 2a). In order to determine the thickness of the bimetallic layer, we compared the sensitivity, reflectivity and resonance angle of different thickness, as shown in Figure 3. In this paper, in order to simplify the process of parameter optimization, the thickness ratio of Au and Ag in the bimetal is set to 1:1.

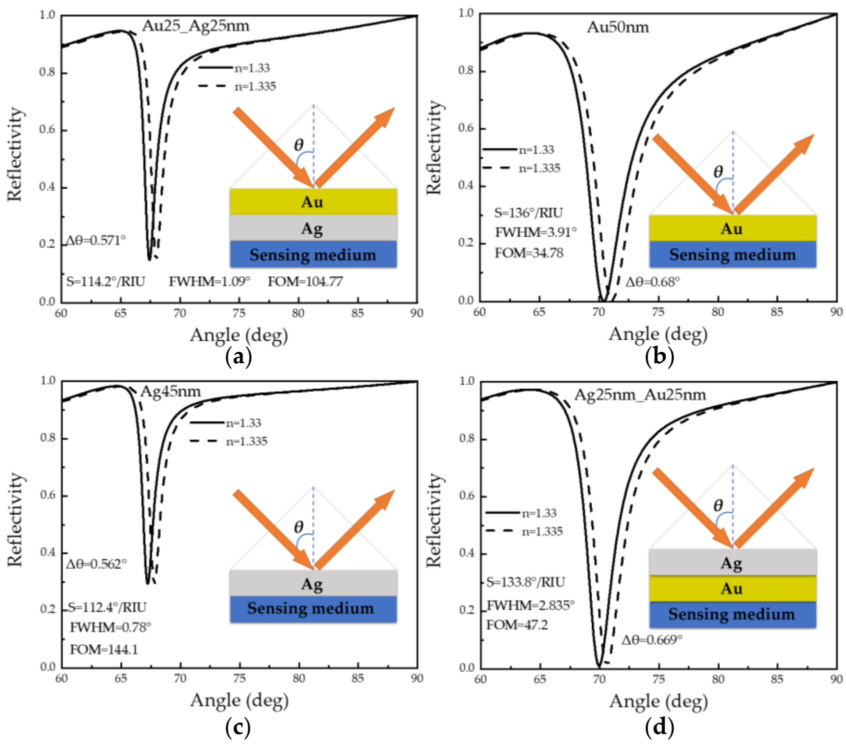

Figure 2. (**a**–**d**) Schematic diagram of SPR sensors with different metal layer and their reflectivity curves and sensing parameters at 632.8 nm: with Au/Ag layer; with Au layer; with Au layer; with Ag/Au layer.

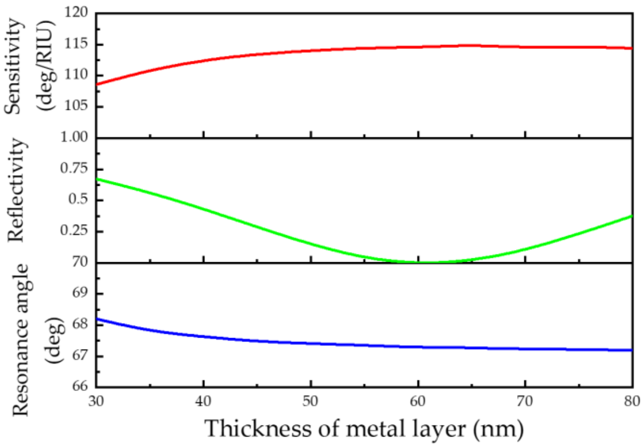

Figure 3. The curves of sensitivity, reflectivity and resonance angle with the thickness of bimetallic layer.

It can be seen from Figure 3 that the sensitivity of the device increases as the thickness of the bimetal layer increases. When the thickness is greater than 50 nm (Au 25 nm, Ag 25 nm), the sensitivity basically remains unchanged. Figure 3 also shows that the absorption peak of the reflectance curve reaches its minimum value at 60 nm of the bimetallic layer and the absorption peak shifts to lower angle with the increase of the thickness of the bimetallic layer. When the thickness is greater than 50 nm (Au 25 nm, Ag 25 nm), the curve is basically flat. In summary, although the reflectivity at a thickness of 60 nm is lower, the metal layer should not be too thick [27]. Other dielectrics will be covered on the Ag surface, to transfer the energy completely to the surface plasmons. Therefore, the thickness of the bimetallic layer needs to be adjusted according to the thickness of the covered silicon layer.

Next, we compare this model with three other common metal structures—namely, bare Au (Figure 2b), bare Ag (Figure 2c), and Au/Ag bimetal (Figure 2d). Figure 2a–d show the changes in the reflectance curves of the four structures mentioned above when the refractive index of the test object changes from 1.33 to 1.335. Figure 2a shows the Au/Ag bimetallic sensor we designed and its sensing characteristics. When the incident angle is about 67.5 degrees, the sensitivity of 114.2°/RIU and the FOM of 104.77 are obtained. Comparing with Figure 2b,d, it can be seen that under the condition of the same metal layer thickness, the above sensing characteristic parameters are obviously better than the Ag/Au bimetallic SPR sensor and bare Au SPR sensor. However, compared with the SPR sensor with bare Ag structure in Figure 2c, the proposed device has no advantages. Therefore, we expect to enhance the sensing performance of the device and prevent the oxidation of the surface Ag layer by covering the Ag layer with high refractive index material silicon.

3.2. Influence of Silicon Layer on SPR Sensor

In the analysis in the previous section, we find that the prism/Au/Ag/medium structure has excellent sensing performance. Due to the easily oxidized nature of Ag, it cannot be directly used as a sensing layer. Therefore, we cover the Ag surface with silicon to prevent the Ag from being oxidized, the refractive index of silicon is 3.874 + 0.016i [28]. In addition, the high refractive index properties of silicon can also improve the sensitivity of SPR sensor. In this section, we will discuss the impact of a silicon overlay on the surface of the Au/Ag bimetallic sensors.

The SPR response of Au/Ag bimetallic layer with different thickness of silicon is studied. In the previous section, when the bimetallic layer is 60 nm, the sensor obtains the minimum reflectivity at resonance, but when the thickness of the bimetallic layer is thicker than 50 nm, the sensitivity of the sensor basically does not change. Considering the silicon layer as a loss material, when it covers the surface of the bimetallic layer, in order to obtain the minimum reflectivity at resonance, the thickness of the bimetallic layer should be appropriately reduced [27]. Figure 4a shows that the reflectivity curve of the sensor with different bimetallic layer thickness covering 6 nm silicon layer, and the reflectivity of the sensor is the lowest when the bimetallic layer thickness is 50 nm. In order to achieve smaller reflectivity—that is, to enhance SPR—the thickness of the bimetallic layer is set to 50 nm.

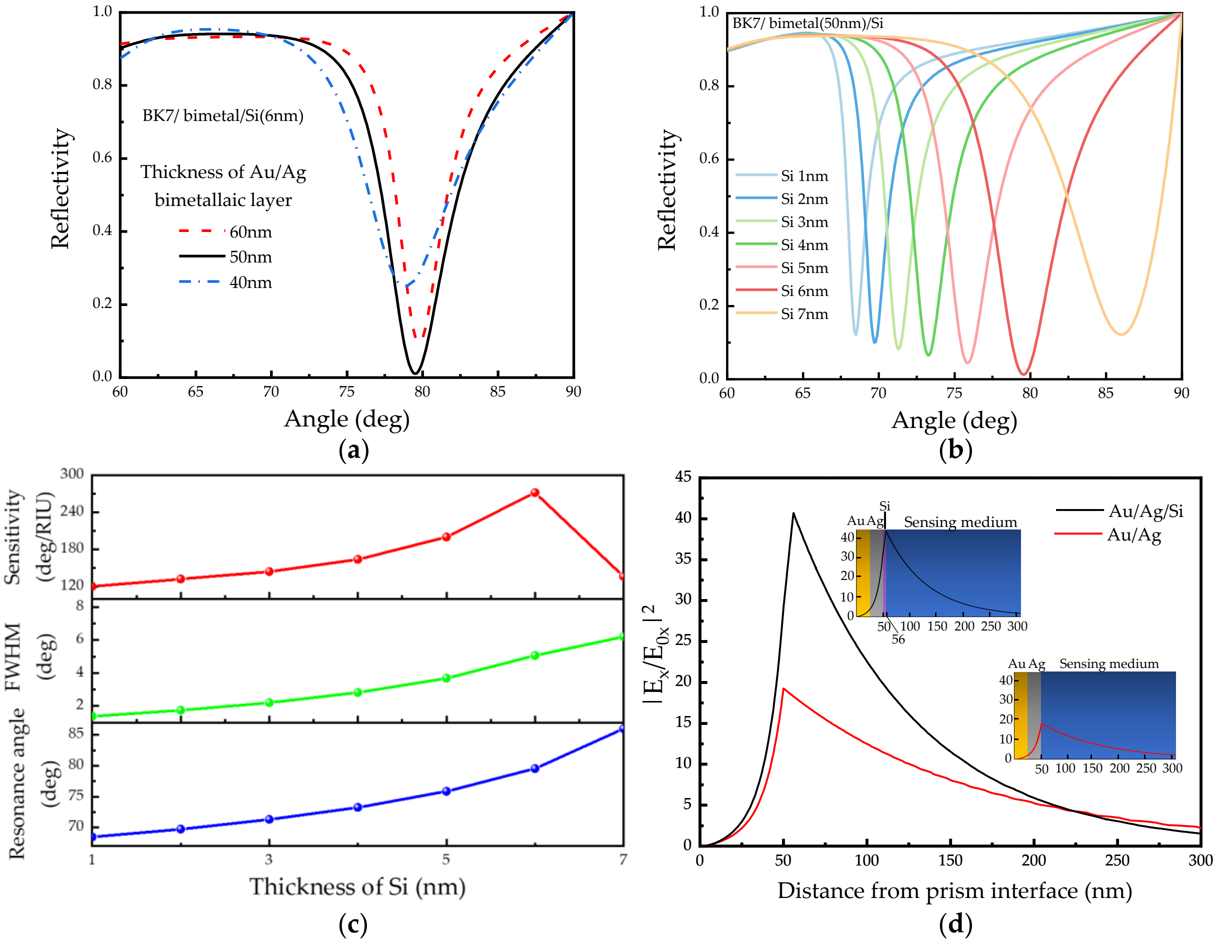

Figure 4. (**a**) Reflectance curves of sensors with different thickness of bimetallic layer covered with 6nm silicon layer; (**b**) When the refractive index of the sensing region is 1.33, the SPR curves with different thickness of Si at 632.8 nm; (**c**) the curves of sensitivity, reflectivity and resonance angle with the thickness of Si layer; (**d**) electric field distributions for the Au/Ag/Si sensor (black line) and Au/Ag sensor (red line), respectively.

The sensitivity reaches the maximum when the thickness of silicon layer is 6 nm, which is 272.6°/RIU, as shown in Figure 4c, FWHM and resonance angle increase with the increase of silicon thickness. The sensitivity of the sensor will be improved by covering the silicon layer, but the FOM will decrease with the increase of FWHM. In addition, a too-large resonance angle is not conducive to experimental operations and will reduce the detection range of the sensor.

The electric field diagram in Figure 4d illustrates this phenomenon. The black line and red line in Figure 4d show the density distribution of the electric field X-component of Au/Ag bimetallic structure (25 nm/25 nm) and Au/Ag/Si structure (25 nm/25 nm/6 nm) in the direction perpendicular to the prism interface, respectively. It can be seen from the illustration that the electric field at the Si/dielectric interface is significantly enhanced relative to the Ag/dielectric interface. In an analyte region, the larger interaction of the electric field leads to the higher sensitivity [29].

Compared with the Ag/Si SPR structure (50 nm/-) under the same conditions, the Au/Ag/Si structure (25 nm/25 nm/-) shows higher sensitivity when covering different thickness silicon layer, as shown in Figure 5. This shows that when the surface of the bimetallic layer is covered with high refractive index material, silicon, the surface field strength of the sensor increases, which makes the sensor surface more sensitive to the change of the refractive index of the detection medium, thus improving the sensitivity.

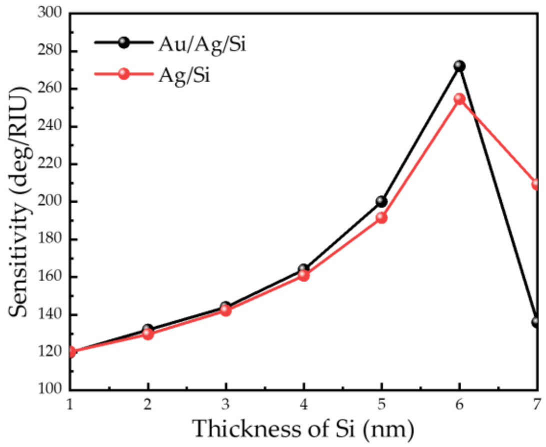

Figure 5. Sensitivity comparison between Au/Ag/Si structure and Ag/Si structure.

3.3. Influence of 2D Materials on SPR Sensor

Due its ultra-high specific surface area and high carrier mobility, 2D materials are often coated on the surface of SPR sensor as sensing layer to improve its sensing performance.

In this section, the influence of 2D materials on the performance of SPR sensors will be discussed.

The performance of the sensor is simulated when several 2D materials cover the surface of the sensor. The refractive index and thickness of the 2D materials are listed in Table 2 [30–32]. From the results discussed in Sections 3.1 and 3.2, we set the thickness of the bimetallic layer to 50 nm, and the thickness of the silicon layer is fine-tuned depending on the 2D material covering it. Considering that the 2D material has a high refractive index real part like silicon, when the 2D material covers the surface of the sensor, the thickness of the silicon layer needs to be adjusted. In order to simplify the research process, the initial thickness of silicon is set to 6 nm. When covering 2D materials with different thicknesses, the thickness of silicon will be appropriately reduced. In order to excite a stronger SPR effect, when the refractive index of the sensing medium is 1.33, the lowest value of the reflectance curve shall not be lower than 0.2. Table 3 optimizes the thickness of graphene and silicon. It can be seen that when the silicon layer is 6 nm and the graphene are two layers, the sensor obtains the maximum sensitivity of 297.2°/RIU. It can be seen from Table 3 that if the number of graphene layers is increased without changing the thickness of silicon layer, the FOM of the sensor will decrease. Furthermore, the sensitivity of the sensor will decrease with the decrease of the thickness of the silicon layer.

Table 2. The main parameters of several 2D materials.

Materials	Thickness of Single Layer (nm)	Refractive Index
MXene	0.993	2.38 + 1.33i
Graphene	0.34	3 + 1.149i
MoS_2	0.65	5.08 + 1.17i

Figure 6a shows the characteristic parameters of the sensor when different thicknesses of graphene are covered on the bare bimetallic layer. It can be seen from Figure 6b that the sensitivity of the sensor is not significantly improved when covering multiple layers of graphene, and the minimum reflectance of the sensor will increase. At the same time, the FOM gradually decreases as the number of graphene layer increases.

Table 3. Sensing characteristics of bimetal/Si/Graphene sensor.

Thickness of Si (nm)	Layer of Graphene	Sensitivity (deg/RIU)	FOM	Rmin
6	1	293.4	45.1	0.02
6	2	297.2	39.75	0.106
6	3	254.4	34.42	0.223
5	3	227.8	34.75	0.094
5	4	234.4	33.04	0.165
5	5	233	32.18	0.241
4	5	200.8	33	0.172
4	6	195.8	30.72	0.225
3	6	175	33.3	0.192
3	7	175.4	30.99	0.31
2	7	153.8	33	0.204
1	7	140.8	37.84	0.179
1	8	141.8	34.7	0.219
0	8	130	39.73	0.203

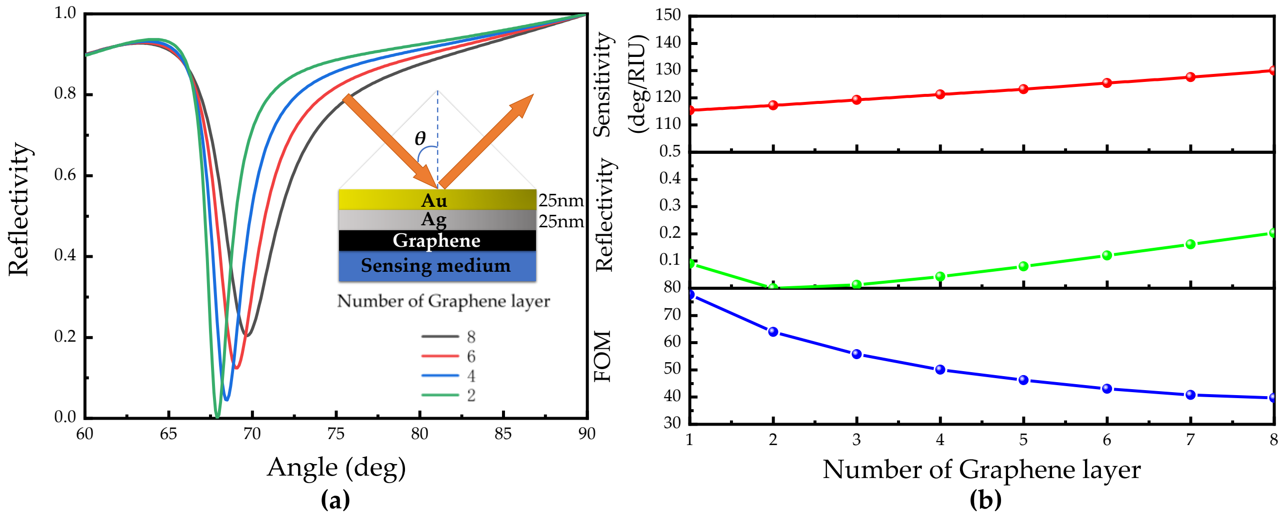

Figure 6. (**a**) Reflectivity curves of graphene sensors with different thickness; (**b**) the curves of sensitivity, reflectivity and FOM with the number of graphene layer.

Similarly, we studied the case of other 2D materials covering the silicon surface, and the optimization process shows the same rules as graphene. After optimization, the sensor has the maximum sensitivity of 274°/RIU when a single layer of MXene is covered on a 6 nm silicon layer. When a single layer of MoS_2 is covered on a 5 nm silicon layer, the sensor has a maximum sensitivity of 246°/RIU. Figure 7 shows the reflectivity curves, FWHM and FOM for the three configurations.

Table 4. Sensitivity analysis of the proposed structure and recently investigated SPR biosensor.

Wavelength (nm)	Structure	Sensitivity (deg/RIU)	FOM	Reported Year and References
633	BK7/Ag/Si/MXene	231	39.83	2020 [18]
632.8	BK7/Au/MoS_2	174.15	27.86	2020 [32]
633	BK7/Ag/Si/BP/MXene	264	41.25	2020 [33]
632.8	BK7/Au/WSe2/Graphene	178.87	27.41	2020 [32]
632.8	BK7/Au/Ag/Si/MXene	274	36.88	This work
632.8	BK7/Au/Ag/Si/MoS_2	246	34.1	This work
632.8	BK7/Au/Ag/Si/Graphene	297.2	39.75	This work

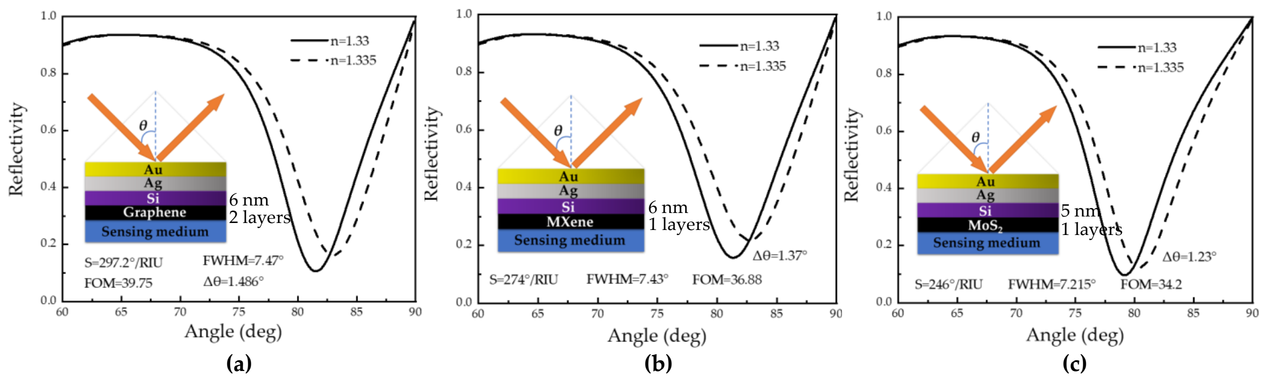

Figure 7. Reflectivity curve and sensing characteristics of the sensor with different thickness of silicon and different kinds of 2D materials on the surface of Au (25 nm) and Ag (25 nm) (**a**) Si (6 nm)/Graphene (2 layer), (**b**) Si (6 nm)/MXene (1 layer), (**c**) Si (5 nm)/MoS_2 (1 layer). Table 4 shows the sensitivity and quality factor of the sensor when the sensor surface is covered with different 2D materials. Compared with the reported structure, the sensitivity of our proposed sensor is obviously higher.

In order to test the detection performance of the sensor, we set the refractive index of the detection medium to 1.33 + $\Delta\theta$ with a step size of 0.001 to simulate the change in the refractive index of the sensor surface from 1.33 to 1.34 during actual measurement. The configuration of the sensor is the structure in Table 4 when the surface is covered with graphene, MXene and MoS_2. Figure 8 shows the change of the absorption peak when the refractive index increases from 1.33 to 1.34. After calculation, the resonance angle change under this configuration has a good linear relationship with the refractive index change; then, the correlation coefficient reaches 0.99. The relationship between the refractive index of the solution n and the resonance angle θ can be expressed as follows:

$$n_1 = \frac{\theta_1 + 312.1}{295.9} (\mathrm{Au/Ag/Si/Graphene}) \tag{9}$$

$$n_2 = \frac{\theta_2 + 275.1}{268} (\mathrm{Au/Ag/Si/MXene}) \tag{10}$$

$$n_3 = \frac{\theta_3 + 265.4}{259} (\mathrm{Au/Ag/Si/MoS_2}) \tag{11}$$

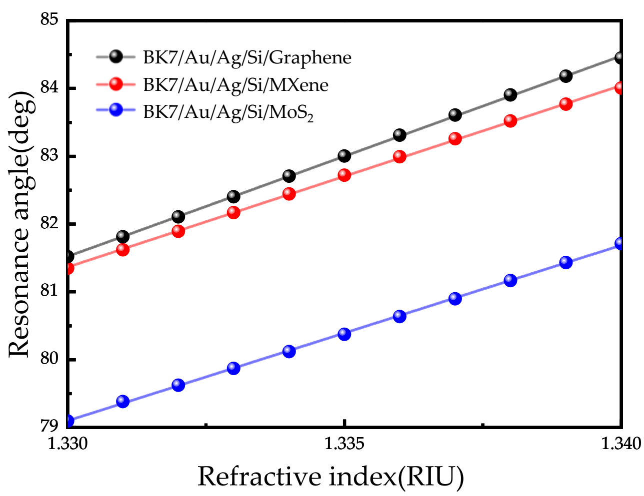

Figure 8. Variation of resonance angle with refractive index of sensors covered with different 2D materials.

It can be seen from Figure 8 and Table 4 that among the three types of sensors, the graphene sensor has the highest sensitivity, while the MoS_2 sensor has a smaller resonance angle. This result is of great significance. In the production of sensors, the thickness of each layer of material is often not very accurate. Therefore, when the thickness of the silicon layer is 5 nm, one layer MoS_2 should be covered on it, and when the thickness of the silicon layer is closer to 6nm, a layer graphene can be considered to be covered on it, which can achieve a better sensing performance.

3.4. Sensing Characteristics in Wavelength Interrogation

In this section, we study the sensing characteristics of the sensor in wavelength interrogation. The silicon layer and the 2D materials limit the distribution of the electric field on the surface of the sensor and improve the sensitivity. On the one hand, the silicon layer and the 2D materials as a loss material will also reduce the reflectivity of the sensor. On the other hand, for longer wavelengths, the field intensity near the bimetallic layer decreases and the penetration depth increases. The increase in penetration depth is due to the fact that the bimetallic layer is a better conductor at longer wavelengths, which leads to a less confined modes at the interface [19]. This allows the dielectric-metal field strength to be enhanced compared to bare metal structures. Taking the configuration of 50 nm gold and silver, 6 nm silicon layer and 2 layers of graphene as an example. We choose 70 degrees, 75 degrees and 80 degrees of incidence angles for comparison. Figure 9b shows the reflectance curve of the sensor under different incident angles in wavelength interrogation. The detection medium is an aqueous solution with a refractive index of 1.333 + Δn. It can be seen that as the incident angle increases, the resonant peak of the sensor is blue-shifted, and the sensitivity and FOM also decrease.

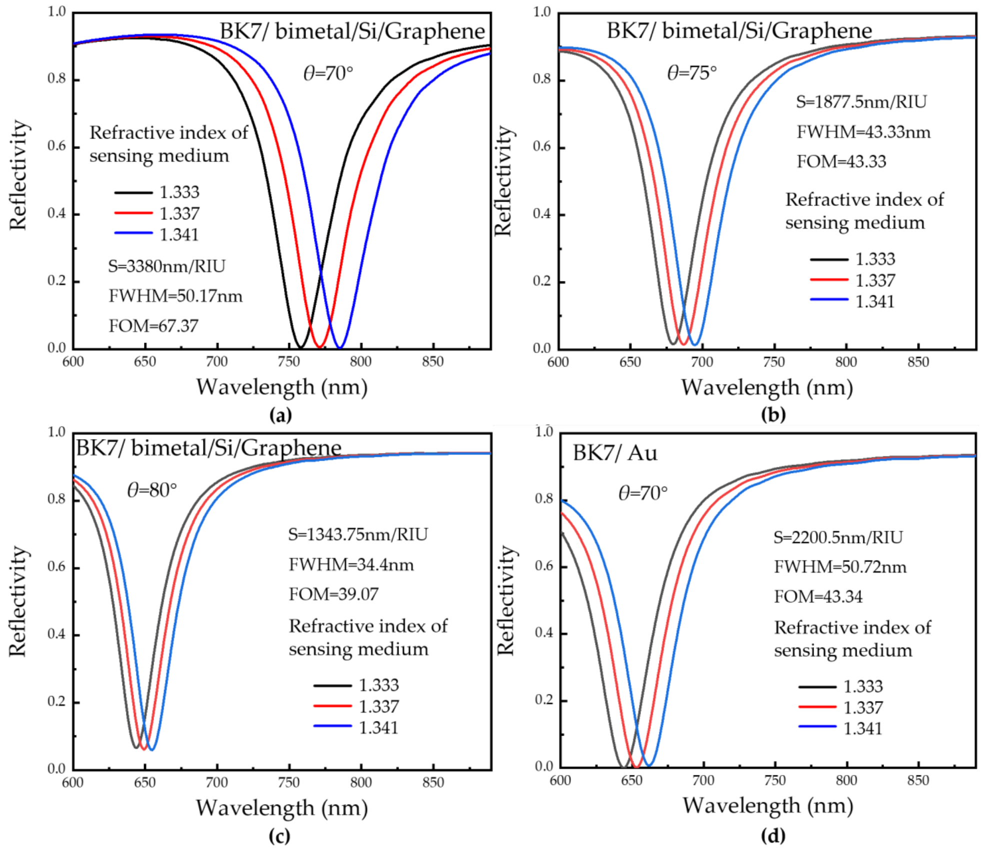

Figure 9. The sensing characteristics in wavelength interrogation at different incident angles (**a**) the incidence angle is 70°; (**b**) the incidence angle is 75°; (**c**) the incidence angle is 80°; (**d**) sensing characteristics of wavelength modulation of Au sensor at incidence angle of 70°.

Compared with Figure 9d, the sensitivity of the proposed sensor is still greatly improved compared with the bare gold layer configuration. It can be seen from Figure 9a that the sensor reaches sensitivity of 3380 nm/RIU when the incident angle is 70°. Compared with the SPR sensor with bare gold layer configuration, the sensitivity is increased by 53.6%.

4. Conclusions

In this paper, a novel SPR biosensor is proposed. By optimizing bimetal layer and silicon layer, the sensor obtains a sensitivity of 272.6°/RIU with 50 nm bimetal layer and 6 nm silicon film. Compared with the traditional SPR sensor, the sensitivity is improved by about 100%. However, the bare silicon layer is not suitable for biosensing. Therefore, we cover the surface of the sensor with several different 2D materials. The unique photoelectric properties and high adsorption energy of these 2D materials enhance the binding of the substance to be detected on the surface of the sensor. When covering MXene, MoS_2 and graphene, the sensitivity of the sensor is 274°/RIU, 246°/RIU, 293.4°/RIU, respectively. The results show that the proposed sensor is very sensitive to small changes in refractive index. Next, we discussed that different kinds of 2D materials can be covered with different thicknesses of silicon layer to achieve excellent sensing characteristics. Finally, the results show that the sensitivity of the proposed Au/Ag/Si/Graphene sensor is 53.6% higher than that of the bare gold sensor. Therefore, the structure has great potential in biosensor, and can be used in biological detection, food safety, medical diagnosis and so on.

Author Contributions: Conceptualization, P.Z. and J.W.; Software, P.Z. and J.W.; validation J.W.; data curation, J.W. and G.C.; writing—original draft preparation, P.Z. and J.W.; writing—review and editing, P.Z., J.W., G.C. and T.T.; supervision, J.S. and C.L.; project administration, J.S. and C.L. All authors have read and agreed to the published version of the manuscript.

Funding: This work was funded by Finance Science and Technology Project of Hainan Province (ZDKJ2020009) and Hainan Provincial Natural Science Foundation of China (2019RC054) and Dongguan Introduction Program of Leading Innovative and Entrepreneurial Talents.

Institutional Review Board Statement: Not applicable.

Informed Consent Statement: Not applicable.

Data Availability Statement: Research data presented in this study are available on request from the corresponding author.

Conflicts of Interest: The funders had no role in the design of the study; in the collection, analyses, or interpretation of data; in the writing of the manuscript, or in the decision to publish the results.

References

1. Cao, Y.; Cao, Y.; Shi, Y.; Cai, Y.; Chen, L.; Wang, D.; Liu, Y.; Chen, X.; Zhu, Z.; Hong, Z.; et al. Surface plasmon resonance biosensor combined with lentiviral particle stabilization strategy for rapid and specific screening of P-Glycoprotein ligands. *Anal. Bioanal. Chem.* **2021**, *413*, 2021–2031. [CrossRef]
2. Zeng, Y.; Hu, R.; Wang, L.; Gu, D.; He, J.; Wu, S.-Y.; Ho, H.-P.; Li, X.; Qu, J.; Gao, B.Z.; et al. Recent advances in surface plasmon resonance imaging: Detection speed, sensitivity, and portability. *Nanophotonics* **2017**, *6*, 1017–1030. [CrossRef]
3. Li, C.-T.; Chen, H.-F.; Un, I.-W.; Lee, H.-C.; Yen, T.-J. Study of optical phase transduction on localized surface plasmon resonance for ultrasensitive detection. *Opt. Express* **2012**, *20*, 3250–3260. [CrossRef]
4. Zhang, P.; Tang, T.; Shen, J.; Luo, L.; Li, C.; Yao, J. Spin Hall effect of light in a prism-waveguide coupling structure with a magneto-optical bimetallic film. *Superlattices Microstruct.* **2019**, *128*, 136–143. [CrossRef]
5. Xu, H.; Wu, L.; Dai, X.; Gao, Y.; Xiang, Y. An ultra-high sensitivity surface plasmon resonance sensor based on graphene-aluminum-graphene sandwich-like structure. *J. Appl. Phys.* **2016**, *120*, 053101. [CrossRef]
6. Miyazaki, C.M.; Shimizu, F.M.; Ferreira, M. Surface Plasmon Resonance (SPR) for Sensors and Biosensors. In *Nanocharacterization Techniques*; Elsevier: Amsterdam, The Netherlands, 2017; pp. 183–200.
7. Kumar, S.; Singh, R. Recent optical sensing technologies for the detection of various biomolecules: Review. *Opt. Laser Technol.* **2021**, *134*, 106620. [CrossRef]

8. Raghuwanshi, S.K.; Kumar, M.; Jindal, S.K.; Kumar, A.; Prakash, O. High-Sensitivity Detection of Hazardous Chemical by Special Featured Grating-Assisted Surface Plasmon Resonance Sensor Based on Bimetallic Layer. *IEEE Trans. Instrum. Meas.* **2020**, *69*, 5072–5080. [CrossRef]
9. Preechaburana, P.; Gonzalez, M.C.; Suska, A.; Filippini, D. Surface Plasmon Resonance Chemical Sensing on Cell Phones. *Angew. Chem. Int. Ed.* **2012**, *51*, 11585–11588. [CrossRef]
10. Zhu, C.; Dong, S. Recent progress in graphene-based nanomaterials as advanced electrocatalysts towards oxygen reduction reaction. *Nanoscale* **2013**, *5*, 1753–1767. [CrossRef]
11. Li, Q.; Dou, X.; Zhang, L.; Zhao, X.; Luo, J.; Yang, M. Oriented assembly of surface plasmon resonance biosensor through staphylococcal protein A for the chlorpyrifos detection. *Anal. Bioanal.Chem.* **2019**, *411*, 6057–6066. [CrossRef]
12. Wu, Q.; Li, N.; Wang, Y.; Xu, Y.; Wu, J.; Jia, G.; Ji, F.; Fang, X.; Chen, F.; Cui, X. Ultrasensitive and selective determination of carcinoembryonic antigen using multifunctional ultrathin amino-functionalized Ti_3C_2-MXene nanosheets. *Anal. Chem.* **2020**, *92*, 3354–3360. [CrossRef]
13. Zhou, J.; Qi, Q.; Wang, C.; Qian, Y.; Liu, G.; Wang, Y.; Fu, L. Surface plasmon resonance (SPR) biosensors for food allergen detection in food matrices. *Biosens. Bioelectron.* **2019**, *142*, 111449. [CrossRef]
14. Ashley, J.; Shahbazi, M.-A.; Kant, K.; Chidambara, V.A.; Wolff, A.; Bang, D.D.; Sun, Y. Molecularly imprinted polymers for sample preparation and biosensing in food analysis: Progress and perspectives. *Biosens. Bioelectron.* **2017**, *91*, 606–615. [CrossRef]
15. Karabchevsky, A.; Tsapovsky, L.; Marks, R.S.; Abdulhalim, I. Study of Immobilization Procedure on Silver Nanolayers and Detection of Estrone with Diverged Beam Surface Plasmon Resonance (SPR) Imaging. *Biosensors* **2013**, *3*, 157–170. [CrossRef] [PubMed]
16. Wu, L.; Chu, H.; Koh, W.; Li, E. Highly sensitive graphene biosensors based on surface plasmon resonance. *Opt. Express* **2010**, *18*, 14395–14400. [CrossRef] [PubMed]
17. Wu, L.; You, Q.; Shan, Y.; Gan, S.; Zhao, Y.; Dai, X.; Xiang, Y. Few-layer Ti3C2Tx MXene: A promising surface plasmon resonance biosensing material to enhance the sensitivity. *Sens. Actuators B* **2018**, *277*, 210–215. [CrossRef]
18. Kumar, R.; Pal, S.; Prajapati, Y.; Saini, J. Sensitivity enhancement of MXene based SPR sensor using silicon: Theoretical analysis. *Silicon* **2020**, *13*, 1–8. [CrossRef]
19. Varasteanu, P. Transition metal dichalcogenides/gold-based surface plasmon resonance sensors: Exploring the geometrical and material parameters. *Plasmonics* **2020**, *15*, 243–253. [CrossRef]
20. Lio, G.E.; Ferraro, A.; Ritacco, T.; Aceti, D.M.; De Luca, A.; Giocondo, M.; Caputo, R. Leveraging on ENZ Metamaterials to Achieve 2D and 3D Hyper-Resolution in Two-Photon Direct Laser Writing. *Adv. Mater.* **2021**, *33*, e2008644. [CrossRef]
21. Garoli, D.; Calandrini, E.; Giovannini, G.; Hubarevich, A.; Caligiuri, V.; De Angelis, F. Nanoporous gold metamaterials for high sensitivity plasmonic sensing. *Nanoscale Horiz.* **2019**, *4*, 1153–1157. [CrossRef]
22. Palermo, G.; Sreekanth, K.V.; Maccaferri, N.; Lio, G.E.; Nicoletta, G.; De Angelis, F.; Hinczewski, M.; Strangi, G. Hyperbolic dispersion metasurfaces for molecular biosensing. *Nanophotonics* **2020**, *10*, 295–314. [CrossRef]
23. Kabashin, A.V.; Evans, P.; Pastkovsky, S.; Hendren, W.; Wurtz, G.A.; Atkinson, R.; Pollard, R.; Podolskiy, V.A.; Zayats, A.V. Plasmonic nanorod metamaterials for biosensing. *Nat. Mater.* **2009**, *8*, 867–871. [CrossRef] [PubMed]
24. Sreekanth, K.V.; Alapan, Y.; ElKabbash, M.; Ilker, E.; Hinczewski, M.; Gurkan, U.A.; De Luca, A.; Strangi, G. Extreme sensitivity biosensing platform based on hyperbolic metamaterials. *Nat. Mater.* **2016**, *15*, 621–627. [CrossRef]
25. Ruffato, G.; Romanato, F.; Garoli, D.; Cattarin, S.J.O.E. Nanoporous gold plasmonic structures for sensing applications. *Opt. Express* **2011**, *19*, 13164–13170. [CrossRef] [PubMed]
26. McPeak, K.M.; Jayanti, S.V.; Kress, S.J.; Meyer, S.; Iotti, S.; Rossinelli, A.; Norris, D.J. Plasmonic films can easily be better: Rules and recipes. *ACS Photonics* **2015**, *2*, 326–333. [CrossRef]
27. Pal, S.; Prajapati, Y.; Saini, J. Analyzing the Sensitivity of Heterostructure of BP-Graphene/TMDC Layer Coated SPR Biosensor. In *Advances in VLSI, Communication, and Signal Processing*; Springer: Berlin, Germany, 2020; pp. 663–671.
28. Green, M.A. Self-consistent optical parameters of intrinsic silicon at 300 K including temperature coefficients. *Sol. Energy Mater. Sol. Cells* **2008**, *92*, 1305–1310. [CrossRef]
29. Shalabney, A.; Abdulhalim, I. Electromagnetic fields distribution in multilayer thin film structures and the origin of sensitivity enhancement in surface plasmon resonance sensors. *Sens. Actuators A* **2010**, *159*, 24–32. [CrossRef]
30. Srivastava, A.; Verma, A.; Das, R.; Prajapati, Y. A theoretical approach to improve the performance of SPR biosensor using MXene and black phosphorus. *Optik* **2020**, *203*, 163430. [CrossRef]
31. Peng, Q.; Wang, Z.; Sa, B.; Wu, B.; Sun, Z. Electronic structures and enhanced optical properties of blue phosphorene/transition metal dichalcogenides van der Waals heterostructures. *Sci. Rep.* **2016**, *6*, 1–10. [CrossRef]
32. Nurrohman, D.T.; Chiu, N.-F. Surface Plasmon Resonance Biosensor Performance Analysis on 2D Material Based on Graphene and Transition Metal Dichalcogenides. *ECS J. Solid State Sci. Technol.* **2020**, *9*, 115023. [CrossRef]
33. Kumar, R.; Pal, S.; Verma, A.; Prajapati, Y.; Saini, J. Effect of silicon on sensitivity of SPR biosensor using hybrid nanostructure of black phosphorus and MXene. *Superlattices Microstruct.* **2020**, *145*, 106591. [CrossRef]